AB PEPTIDES AND THE EXPOSURE OF THEIR HYDROPHOBIC RESIDUES UPON COPPER(II) COMPLEX FORMATION: PROBING MECHANISMS OF AMYLOID PLAQUE FORMATION IN HUMAN AND RAT PEPTIDE COMPLEXES

by

Sarah N. Sipe

A Senior Honors Project Presented to the

Honors College

East Carolina University

In Partial Fulfillment of the

Requirements for

Graduation with Honors

by

Sarah N. Sipe

Greenville, North Carolina

April 2015

Approved by:

Anne M. Spuches, PhD

Department of Chemistry, East Carolina University

Table of Contents

1. Abstract

Alzheimer's Disease (AD) is a progressive, neurodegenerative disease that affects 35 million people worldwide and is the 6th leading cause of death in the United States. AD is characterized by neurofibrillary tangles and amyloid plaques in the brain. The plaques are formed when amyloid beta (Aβ) peptides aggregate at their hydrophobic residues. Elevated concentrations of essential metals, copper, iron, and zinc, have been detected in the plaques and research indicates that the presence of metals speed up the formation of the plaques.

Previous binding studies have determined that metal binding occurs within the first 16 amino acids of the Aβ peptide, which can be either 40 or 42 amino acids long. The rat Aβ peptide differs by only three amino acid point substitutions and are immune to aggregation. Based on previous thermodynamic binding studies, the exposure of the peptides' hydrophobic residues when bound to copper (II) are hypothesized to be more exposed in the human peptide than the rat. To test this hypothesis, rat and human Aβ28 peptides are probed with hydrophobic fluorophore 1,8-ANS. Increased fluorescence is expected of human Aβ28 if the hydrophobic residues of the peptide-copper complexes are indeed more exposed.

2. Alzheimer's Disease

The well-known devastation of Alzheimer's Disease (AD) paired with the mystery surrounding the disease has made it a popular research topic across many scientific fields. AD is the sixth leading cause of death in the United States with approximately 36 million cases worldwide [1-3]. It is a progressive, neurodegenerative disease that accounts for the majority of dementia cases [1]. AD causes loss of neurons in the cerebral cortex and the brain to atrophy,

which leads to loss of cognitive function, memory, behavioral and physical ability, and ultimately loss of life [2-4].

AD is characterized by amyloid plaques, the primary constituent of which is the amyloid-β (Aβ) peptide [2-8], and neurofibrillary tangles, comprised from hyper phosphorylated tau protein [2-4, 6,]. The physical effect of the plaques and tangles are visible in **Figure 1** [1]. The significance of the rat Aβ peptides is that, though they are produced similarly to the human peptide and differ by only three point substitutions, they do not aggregate to form amyloid plaques [8].

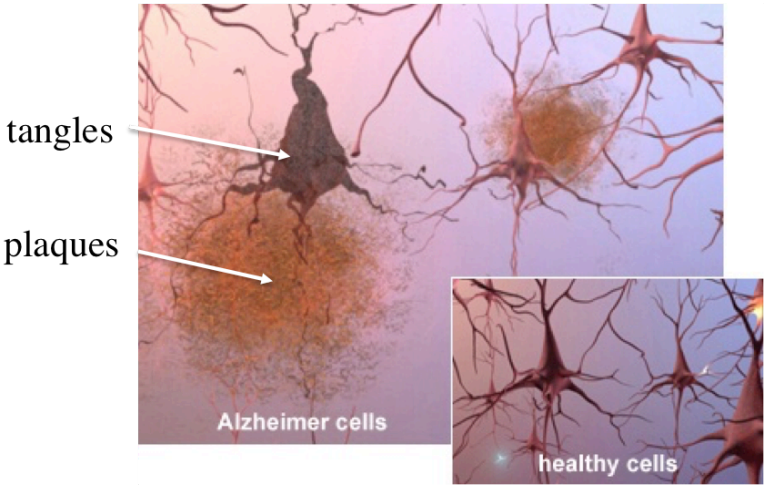

Figure 1. Figure of healthy neurons in the brain (inset) and neurons affected by Alzheimer's disease plaques and tangles [1].

2.1 Amyloid-β

The Aβ peptide is derived from the cleavage of the amyloid precursor protein (APP) from the outer cell membrane or mitochondrial membrane [3, 4, 8]. APP is cleaved by either α-, β-, or γ-secretase [3, 6, 9], the latter of which results in Aβ peptides between 39 and 43 amino acids in length with the most common being 40 and 42 [2-9]. The sequence of human Aβ42 with

the hydrophobic residues highlighted in green and the metal binding histidine residues highlighted in blue is as follows in **Scheme 1.**

DAEFRHDSGYEVHHQKLVFFAEDVGSNKGAIIGLMVGGVVIA

Scheme 1. Sequence of Human Aβ peptide

The rat Aβ42 with highlighted hydrophobic and metal-binding residues with its three point substitutions in red is as follows in **Scheme 2.**

DAEFGHDSGFEVRHQKLVFFAEDVGSNKGAIIGLMVGGVVIA

Scheme 2. Sequence of Human Aβ peptide

The 42 amino acid long peptide is more prone to aggregation into oligomers then further into the amyloid plaques [3-5, 9]. The amyloid cascade hypothesis suggests that this aggregation occurs at the hydrophobic residues (**Figure 2**) and that these aggregates or plaques cause neural dysfunction. This dysfunction leads to incorrect processing of the tau protein, which leads to the formation of the neurofibrillary tangles [3, 9].

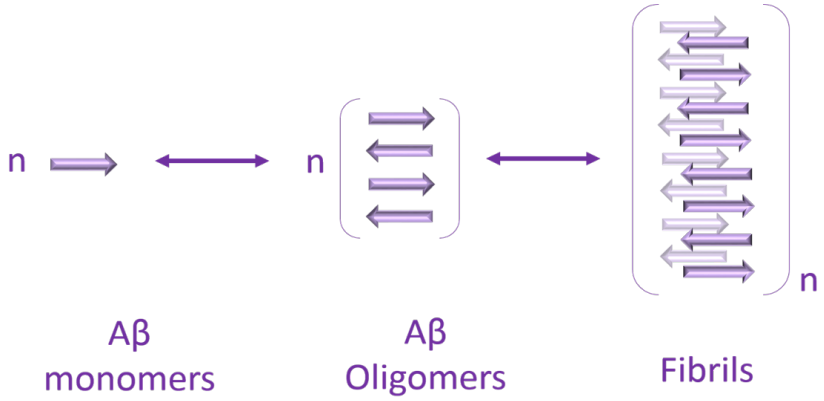

Figure 2. Figure representing the formation of Aβ monomers, oligomers and fibrils. [3-5, 9].

Elevated concentrations of essential metals, copper, zinc, and iron, have been detected in the plaques and are known to enhance aggregation [3-5, 7]. The three histidine residues within the Aβ peptide play a role in the peptide's ability to bind metals within the first 16 amino acids [3, 4]. The metal ion hypothesis of AD pathogenesis suggests that the imbalance in metal homeostasis is the underlying precursor to amyloid plaque formation [3].

A third hypothesis for the pathogenesis of AD competing with the amyloid cascade and metal ion hypotheses is the oxidative stress hypothesis [3]. It states that oxidative stress from reactive oxygen species causes gene defects, leading to neurodegeneration, and ultimately plaque aggregation and subsequent neurological disorders [3].

2.2 Previous thermodynamic studies

As previously noted, copper (Cu^{2+}) can bind to Aβ within its first 16 amino acid residues. Thermodynamic studies into Cu^{2+} binding to Aβ involving the determination of binding constants and changes in enthalpy (ΔH), entropy (ΔS), and overall Gibb's free energy (ΔG) have been conducted in the Spuches lab group using isothermal titration calorimetry [4, 10]. Though the ΔH and TΔS of Cu^{2+} binding to human and rat Aβ28 peptides varied slightly (**Figure 3**), the ΔG for each, which indicates spontaneity or favorability of a reaction, were identical: -6.5 ± 0.2 and -6.3 ± 0.1 kcal/mol at 37°C respectively [4, 10].

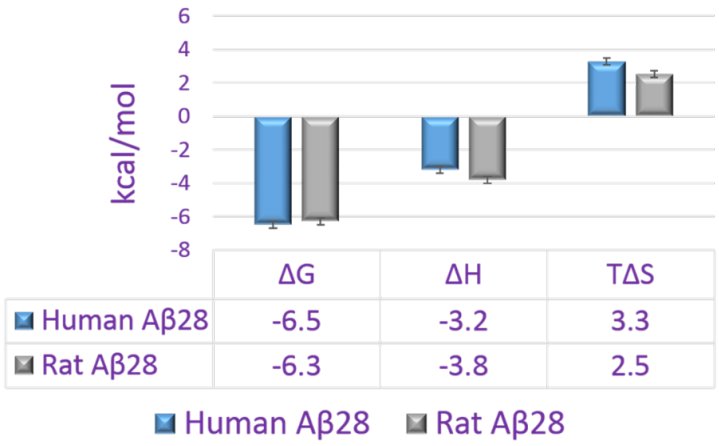

Figure 3. Thermodynamic parameters for Cu^{2+} binding to human and rat Aβ28 [10]. All samples contained 20 mM ACES Buffer (pH = 7.4), 0.1 M NaCl and run at 37 °C.

For further elucidation of how the metal and peptide are binding, the heat capacity of the reactions were determined [10]. Heat capacity (C_p) is a measure of the heat required to raise the temperature of a system by one degree. Typically, a negative C_p value for protein binding is indicative of more buried hydrophobic surfaces [10, 12].

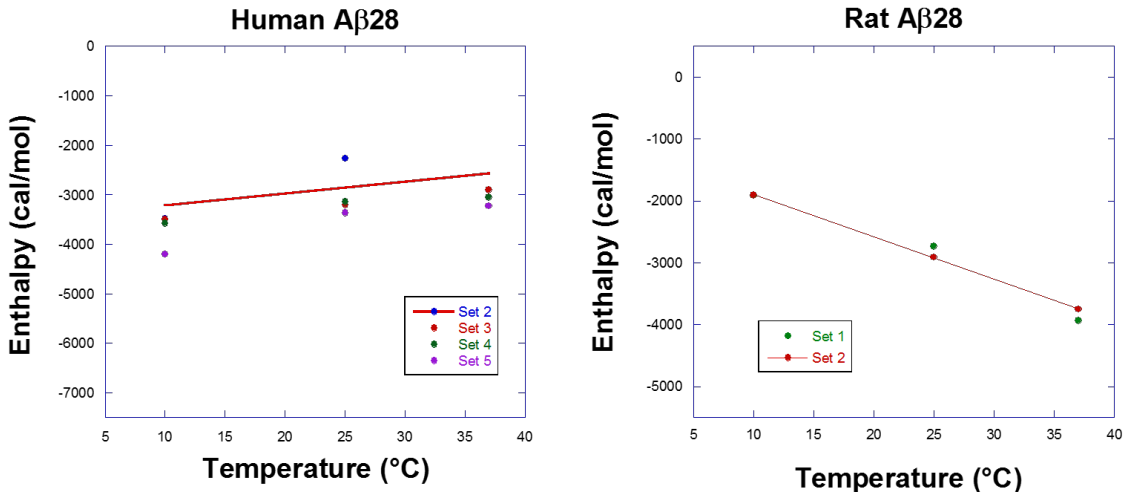

Figure 4. Change in enthalpy as a function of temperature for human and rat Aβ with 2.1 mM Cu^{2+} [10]. Samples contained 20 mM ACES Buffer (pH = 7.4), 0.1 M NaCl. and reactions were conducted at 37 °C.

The C_p of human and rat Aβ28 was determined from the linear slope of ΔH versus temperature (T) shown in **Figure 4** [10]. Their values were determined to be 25 ± 3 and -71 ± 1 cal/mol·°C for human and rat peptide respectively. Based on the much more negative heat capacity of rat Aβ28 binding Cu^{2+}, the hydrophobic residues of the rat peptide are hypothesized to be more buried within the metal-peptide complex than the human as depicted in **Figure 5** [10]. To test this hypothesis, the human and rat complexes were probed with a hydrophobic fluorophore.

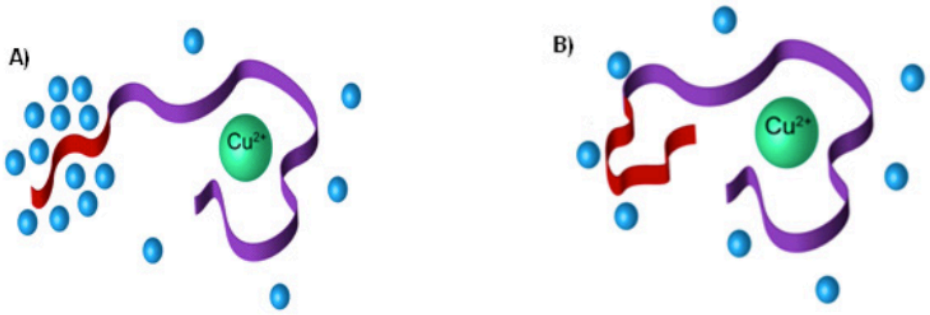

Figure 5. Proposed structures of the metal-peptide complex of A) human Aβ28 and B) rat Aβ28 [10].

3. Fluorometry

Fluorescence along with phosphorescence make up the two categories of luminescence, which encompasses any light that is emitted by a compound from an electronically excited state [13]. In fluorescence, paired and opposite-spin electrons are excited to a single state electronic level (S_1) before decaying back down to the ground state (S_0). In phosphorescence, same-spin electrons are excited to a triplet state (T_1) [13]. The Jablonski diagram in **Figure 6** displays the excitation, decay, and emission of fluorescence and phosphorescence compared to absorption [13]. Not all molecules fluoresce, because once excited, a molecule will return to the ground state in the quickest manner possible. The lifetime of fluorescence is about 10^{-8} seconds whereas

the lifetime of absorbance is shorter, 10^{-15} seconds, and thus preferred [13]. Rigid, aromatic compounds are often fluorescent because there is less flexibility, meaning less possible vibrational relaxation as in absorption.

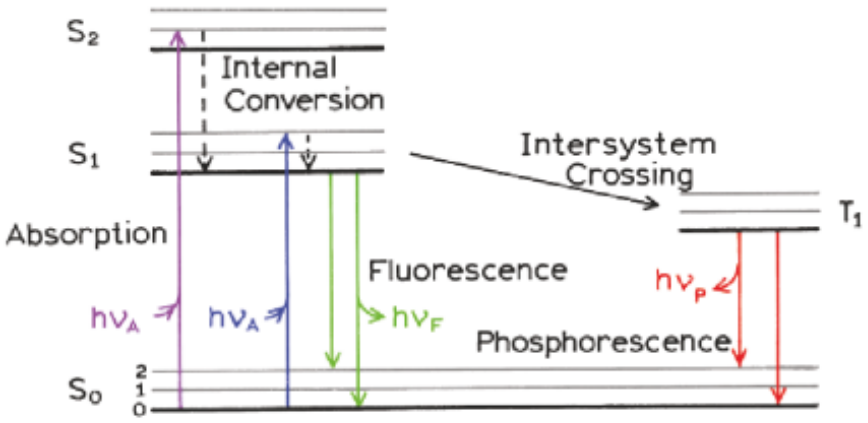

Figure 6. Simple Jablonski diagram of absorption, fluorescence, and phosphorescence. [13].

A distinct characteristic of fluorescence is that it emits light energy at longer wavelengths than the wavelength at which it was excited. Typical absorption spectra of two fluorescent molecules are displayed in **Figure 7** [13]. This lower-energy emission is referred to as the Stokes shift [13]. The Stokes shift is mostly a result of rapid energy loss to the lowest vibrational level within the excited electronic level (S_1) [13]. Fluorescent molecules also tend to decay to higher vibrational levels within the ground state (S_0).

Other causes of the Stokes shift may include solvent effects, reactions that take place at the excited state, and energy transfer [13]. Another effect of fluorescent molecules' rapid relaxation at their excited states is that the emission spectrum of a particular fluorophore is

independent of excitation wavelength; if excited to a higher electronic or vibrational level, the excess energy is quickly dissipated [13].

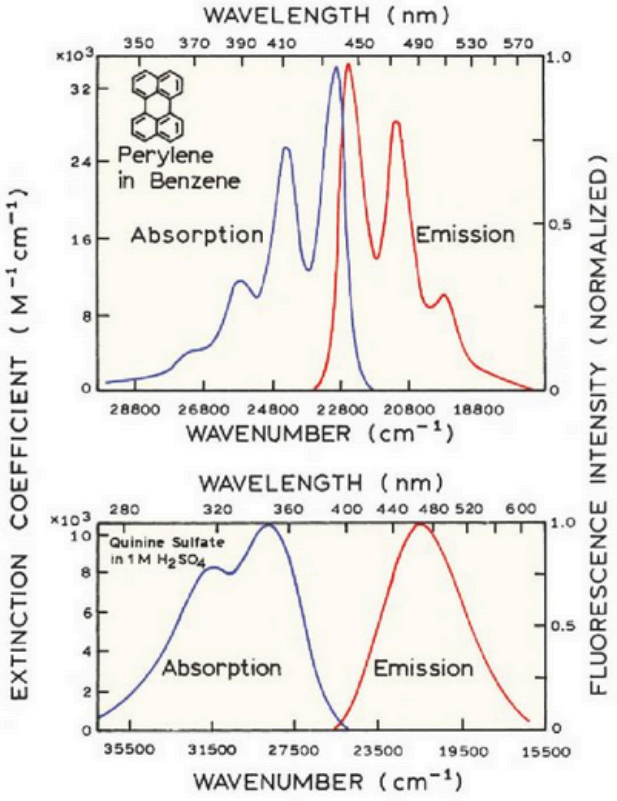

Figure 7. Absorption and emission of perylene (top) and quinine (bottom) [13].

Though the emission spectrum of a fluorophore is independent of excitation, changes in λ_{max} and intensities may still arise from changes in environment. A shift of the λ_{max} to the left to a shorter wavelength is known as a blue shift [13]. A shift of the λ_{max} to the right of a fluorescence spectrum to a longer wavelength is referred to as a red shift [13]. A red shift may occur in polar solvents because the excited electrons may be able to resonate before relaxing, causing it to emit light at a lower and more stable energy. For example, the indole group of

tryptophan displays a blue shift when buried within a protein and red shift when the protein is unfolded [13].

The decrease in fluorescence intensity of a fluorophore is called quenching [13]. Quenching is the process in which a fluorophore in an excited state returns to the ground state without emitting light. This process may occur via dynamic/collisional or static quenching. Dynamic or collisional quenching occurs from diffusive encounters with another molecule in solution, which would act as a quencher. Static quenching is a result of the formation of a non-fluorescent compound from a fluorophore and a quencher. A fluorophore that is free in solution is generally more sensitive to quenching than one that is buried within a macromolecule [13].

4. Project Objectives

The thermodynamic findings from the previous work conducted in the Spuches lab suggested that the rat Aβ28 might have a more compact metal-peptide complex with Cu^{2+} as observed in **Figure 3** [10]. A more compact structure would provide some explanation for why the rat Aβ peptide does not aggregate at its hydrophobic residues like the human Aβ peptide. The aggregation of the human peptide can lead to the formation of the amyloid plaques that the rat peptides do not form. As a means of supporting this hypothesis, a hydrophobic fluorophore 1,8-ANS, was used to probe human and rat Aβ28 peptides that were free in solution and complexed to Cu^{2+}. If the rat complex is more compact than the human, the fluorescent probe should show a more decreased intensity in its presence.

5. Materials

All solutions in this experiment were prepared with a buffer that consisted of 20 mM *N*-(2-Acetonido)-2-aminoethansulfonic acid (ACES, Sigma-Aldrich, St. Louis, MO) and 100 mM sodium chloride (NaCl) in 18 MΩ deionized water. Sodium hydroxide was added to reach a pH of 7.4. A 5mM Cu^{2+} stock was also prepared with 20 mM ACES and 100 mM NaCl (pH 7.4). The fluorophore used as a fluorescent hydrophobic probe in this experiment was 1-Anilinonaphthalene-8-sulfonic acid, (1,8-ANS), which can be seen in **Figure 8**, was ordered from Life Technologies (Carlsbad, CA). The fluorophore solution was prepared by dissolving it in 0.5000 mL of the buffer and 0.5000 mL of dimethylsulfoxide (DMSO). Its concentration was determined from its absorbance at 350 nm ($\varepsilon = 5000\ M^{-1}cm^{-1}$) using a Thermo Scientific NanoDrop 200C spectrophotometer (Waltham, MA).

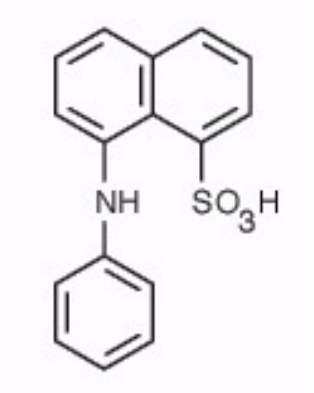

Figure 8. Structure of 1,8-ANS from LifeTechnologies.com

5.1. Peptide purification

Crude Aβ peptides were ordered from the Keck Biotechnology Resource Laboratory (Yale University, New Haven, CT). This length of the peptide was chosen to be 28 amino acids because it contains the residues involved in metal binding and one of the prominent hydrophobic

patches. Full length (40 or 42 amino acids) was not used because of the possibility for aggregation within the time the tests were conducted. The truncated forms of the peptides are depicted in **Scheme 3**.

Human Aβ: DAEFRHDSGYEVHHQKLVFFAEDVGSNK

Rat Aβ: DAEFGHDSGFEVRHQKLVFFAEDVGSNK

Scheme 3. Sequence of human and rat Aβ peptides 1-28.

The peptides were purified with BioLogic DuoFlow HPLC with UV-Vis detector (Bio-Rad, Hercules, CA) utilizing a Vydac Protein and Peptide C18 column (Grace Davison Discover Sciences, Columbia, MD). A gradient flow was utilized with 80% acetonitrile, 19.95% 18 MΩ deionized water, and 0.05% trifluoroacetic acid as solvent A and 99.95% 18 MΩ deionized water and 0.05% TFA as solvent B. Approximately 10 mg of the peptide was dissolved in DMSO and diluted with water. Sonication was necessary to completely dissolve the peptides. The solutions were filtered with a Whatman 0.45 µm filter-tip syringe (GE Healthcare, Pittsburgh, PA). The method used for the purification of the human and rat peptides can be seen in Table 1.

Table 1. Method utilized in the purification of rat and human peptides. Solvent A is 80% acetonitrile, 19.95% 18 MΩ deionized water, and 0.05% TFA. Solvent B is 99.95% 18 MΩ deionized water and 0.05% TFA.

Step	Volume	Description	Parameters	
1	0.00 mL	Isocratic Flow	5% Solvent A 95% Solvent B	10.00 $^{mL}/_{min}$ 50.00 mL
2	50.00 mL	Inject Sample	5% Solvent A 95% Solvent B	10.00 $^{mL}/_{min}$ 10.00 mL
3	60.00 mL	Zero Baseline		
4	60.00 mL	Linear Gradient	5% → 70% Solvent A 95% → 30% Solvent B	10.00 $^{mL}/_{min}$ 350.00 mL
5	410.00 mL	Linear Gradient	70% → 100% Solvent A 30% → 0% Solvent B	10.00 $^{mL}/_{min}$ 30.00 mL
6	440.00 mL	Isocratic Flow	100 % Solvent A 0% Solvent B	10.00 $^{mL}/_{min}$ 20.00 mL
7	460.00 mL	Linear Gradient	100% → 5% Solvent A 0% → 95% Solvent B	10.00 $^{mL}/_{min}$ 50.00 mL
8	510.00 mL	Isocratic Flow	5% Solvent A 95% Solvent B	10.00 $^{mL}/_{min}$ 10.00 mL
9	560.00 mL	End Protocol		

After collection, the peptide solution was flash frozen and lyophilized with a Labconco FreeZone 2.5 (Kansas City, MO) to sublimate the solvent from the peptide. The remaining peptide was dissolved in ACES buffer to determine its concentration from its absorbance. The presence of tyrosine in the human peptide (ε = 1410 $cm^{-1}M^{-1}$ at 280 nm) made concentration determination possible. The tyrosine in the human peptide is substituted for phenylalanine in the rat (ε = 195 $cm^{-1}M^{-1}$ at 257.5 nm). Because there is a total of 4 phenylalanine residues present in rat Aβ, the concentration of the amino acid was divided by 4 to calculate the concentration of the entire peptide.

5.2. Sample Preparation

All samples were prepared in the 20 mM ACES Buffer (pH = 7.4), 0.1 M NaCl. Each sample contained equal concentrations of peptide and fluorophore and the copper solution was 1.5 times that of the peptide. Two controls were prepared to compare against the peptides of interest. The first was the spectrum of 1,8-ANS in buffer and the second took into account the quenching power of free Cu^{2+}. The spectra of each peptide alone and in the Cu^{2+} complex were also gathered. The contents and concentrations of each sample are displayed in **Table 2**. Samples 4 and 6 consisting of the human and rat complexes were incubated for 2.5 hours at a temperature of 37°C.

Table 2. Contents of all samples run in fluorometer. Samples contained 20 mM ACES Buffer (pH = 7.4), 0.1 M NaCl and incubated at 37 °C.

Sample	Content
1	124 μM 1,8-ANS
2	124 μM 1,8-ANS 186 μM Cu^{2+}
3	124 μM Human Aβ 124 μM 1,8-ANS
4	124 μM Human Aβ 124 μM 1,8-ANS 186 μM Cu^{2+}
5	124 μM Rat Aβ 124 μM 1,8-ANS
6	124 μM Rat Aβ 124 μM 1,8-ANS 186 μM Cu^{2+}

The spectra were gathered with a Photon Technology International (PTI) QuantaMaster Fluorometer System (Monmouth Junction, NJ). Excitation was set at 375 nm and each sample's emission was scanned from 400 to 700 nm three times per sample in increments of 1 nm every

0.25 seconds. The peaks were integrated from 400 to 680 nm with the PTI Felix32 software to obtain the peak areas. To obtain peak maximums (λ_{max}), the curves were differentiated by the spectral processing program to obtain linear equations. The x-intercept of the line was recorded as the λ_{max} of each sample.

6. Results and Discussion

The spectra of all six samples are displayed in **Figure 9**. A summary of the intensity and λ_{max} of each sample is presented in **Table 3**. The Cu^{2+} buffer solution did display some quenching power noted by the 4.4% decrease in intensity. However, this effect was minimal and not considered to cause much interference based on the much larger intensities displayed by the introduction of peptide. Furthermore, the presence of "free" Cu^{2+} is even more reduced in the metal-peptide complex solutions due to binding to the peptide.

The spectra of the human Aβ28 peptide with probe and in complex with Cu^{2+} (**Figure 9A**) display a blue shift from the controls. The blue shift of the free peptide from the controls indicates that the probe was in a more hydrophobic environment upon excitation. This blue shift is observed in the free and complexed rat Aβ28 peptide as well (**Figure 9B)**, however two important differences are noted.

First, the intensity of the fluorophore observed in the rat peptide is greater than the intensity observed in the human peptide. This would suggest that the rat peptide has more exposed hydrophobic residues than the human peptide and indeed the rat has two additional hydrophobic residues than the human, with two of these near the Cu^{2+} binding site. The second difference is that the blue shift is much larger for the rat than the human again indicating a more hydrophobic environment. Taken together, we believe that the rat peptide has more structure in

solution than the human peptide and that these residues have formed a hydrophobic patch or pocket thus creating a more hydrophobic environment.

Upon complexation with Cu^{2+}, the fluorophore displayed a decrease in intensity with both human and rat peptides. This decrease is likely the result of dynamic quenching as a consequence of more probe in solution rather than in the presence of hydrophobic amino acid residues. This quenching reveals that the metal-peptide complex of human and rat Aβ28 has a more compact structure than unbound peptide. A larger decrease in intensity is exhibited by the fluorophore from free rat Aβ28 to the metal-peptide complex (50.5%) than from the free human to its complex (21.4%). From this trend, the conformational change in the rat peptide is believed to be more pronounced than the human.

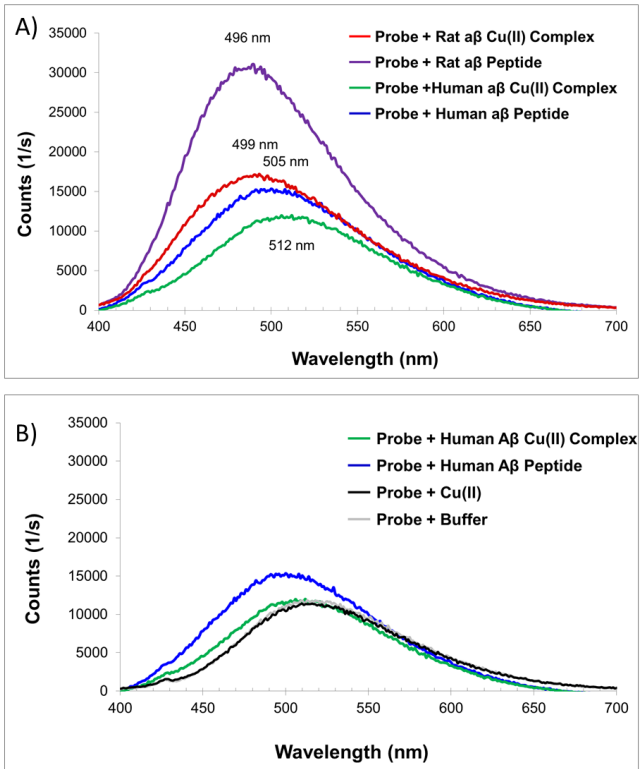

Figure 9. Spectra of the controls, probe (black) and probe plus Cu^{2+} (grey) are displayed in both A and B. Human peptide with probe (blue) and with Cu^{2+}plus probe (green) are displayed in A. Rat peptide with probe (purple) and with Cu^{2+} plus probe (red) are displayed in B. All samples contained 20 mM ACES Buffer (pH = 7.4), 0.1 M NaCl.

Table 3. Summary of fluorometry data.

Peptide/Complex Sample	λ_{max} (nm)	Intensity Decrease
Probe + Human Aβ28	505	21.4%
Probe + Human Aβ28 + Cu(II)	512	
Probe + Rat Aβ28	496	50.5%
Probe + Rat Aβ28 + Cu(II)	499	
Probe	520	4.4%
Probe + Cu(II)	520	

7. Conclusions

The fluorometric spectra of human and rat Aβ28 peptides free in solution and complexed with Cu^{2+} were collected in this experiment. The results support the hypothesis that, upon binding Cu^{2+}, the rat peptide takes on a more compact structure as displayed in **Figures 5** and **10**. The larger decrease in intensity from free peptide to complex was the greatest determining factor of this conclusion in correlation to intensity trends stated by Lakowicz [13]. The slight red shift from free peptide to complexed also corroborates this conclusion.

The more compact structure taken on by the rat Aβ28 peptide makes its hydrophobic residues less exposed than the human. From previous studies, it is known that aggregation occurs at the hydrophobic residues of the human Aβ peptide to form amyloid plaques, which are not detected in rats as displayed in **Figure 10** [3, 5, 8, 9]. The results of this experiment suggest that the lack of amyloid plaques in rats is due to the decrease in exposure of their Aβ peptides' hydrophobic residues upon Cu^{2+} complexation, which in turn prohibits oligomer and fibril formation at the hydrophobic residues.

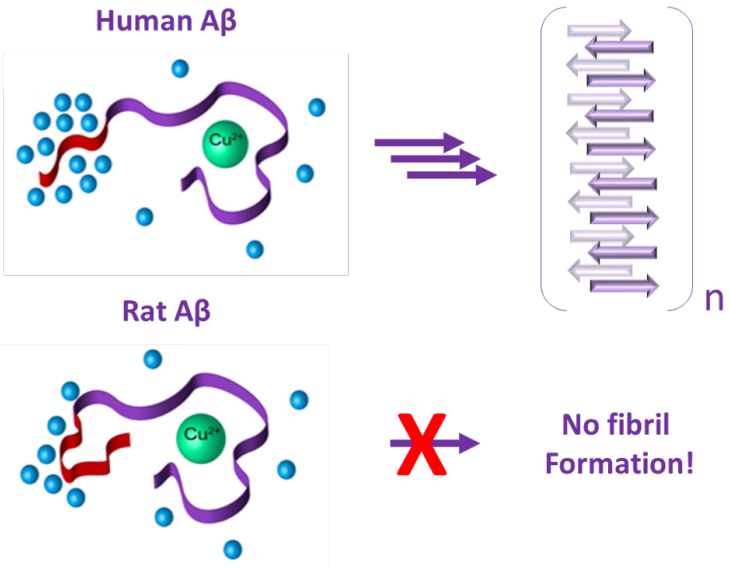

Figure 10. Pictorial representation of human Aβ complex undergoing fibril formation as a result of exposed hydrophobic residues while the more compact rat Aβ complex does not due to buried residues.

8. References

[1] Alzheimer's Association Homepage. http://www.alz.org/

[2] Rafii, M.; Aisen, P. Advances in Alzheimer's Disease Drug Development, *BMC Medicine* **2015**, *13:62*.

[3] Kepp, K. P. Bioinorganic Chemistry of Alzheimer's Disease. *Chem. Rev.* **2012***, 112*, 5193-5239.

[4] Sacco, C.; Skowronsky, R.; Gade, S.; Kenny, J.; Spuches, A. Calorimetric invesitagtion of copper (II) binding to Aβ peptides: thermodynamics of coordination plasticity. *J. Biol. Inorg. Chem.* **2012**, *17:1*.

[5] Olofsson, A.; Linghagen-Persson, M.; Vestling, M.; Sauer-Eriksson, E.; Öhman, A. Quenched hydrogen/deuterium exchange NMR characterization of amyloid-β peptide aggregates formed in the presence of Cu^{2+} or Zn^{2+}. *FEBS Journal* **2009**, *276*, 4051-4060.

[6] Rogaeva, E. The solved and unsolved mysteries of the genetics of early-onset Alzheimer's disease. *NeuroMolecular Medicine* **2002***, 2*, 1-10.

[7] Syme, C.; Nadal, R.; Rigby, S.; Viles, J. Copper binding to the Amyloid-β (Aβ) Peptide Associated with Alzheimer's Disease. *J. Biol. Chem.* **2004**, *279*, 18169-18177.

[8] Hong, L.; Carducci, T.; Bush, W.; Dudzik, C.; Millhauser, G.; Simon, J. Quantification of the Binding Properties of Cu^{2+} to the Amyloid-Beta Peptide: Coordination Spheres for Human and Rat Peptides and Implication of Cu^{2+}-Induced Aggregation. *J. Phys. Chem.* **2010**, *114*, 11261-11271.

[9] Liu, R.; McAllister, C.; Lyubchenko, Y.; Sierks, M. Residues 17-20 and 30-35 of Beta-Amyloid Play Critical Roles in Aggregation. *J. Neurosci.* **2004**, *75*, 162-171.

[10] Gade, S. Cu^{2+} Binding to Aβ peptides: Detailed Heat Capacity Studies Provide Structural Insight into Complex Formation. Masters Thesis, East Carolina University, Greenville, NC, 2013.

[11] Onderka, B. The Heat Capacity of Bismuth Silicates. *Thermochimica Acta* **2015**, *601*, 68-74.

[12] Schönbeck, C.; Holm, R.; Westh, P.; Peters, G. Extending the Hydrophobic Cavity of β-cyclodextrin results in more negative heat capacity changes but reduced binding affinities. *J. Incl. Phenom. Macrocycl. Chem.* **2013**, *78*, 351-361.

[13] Lakowicz, J. *Principles of Fluorescence Spectroscopy*, 3rd Ed.; Springer Science + Business Media, LLC: New York, 2006.